Effects of spatial frequency distributions on amplitude death in an array of coupled Landau-Stuart oscillators

Ye Wu,[1,3] Weiqing Liu,[2,*] Jinghua Xiao,[1,3] Wei Zou,[4,5,6] and Jürgen Kurths[5,6,7]

[1]*State Key Lab of Information Photonics and Optical Communications, Beijing University of Posts and Telecommunications, Beijing 100876, China*

[2]*School of Science, Jiangxi University of Science and Technology, Ganzhou 341000, People's Republic of China*

[3]*School of Science, Beijing University of Posts and Telecommunications, Beijing 100876, People's Republic of China*

[4]*School of Mathematics and Statistics, Huazhong University of Science and Technology, Wuhan 430074, China*

[5]*Institute of Physics, Humboldt University Berlin, Berlin D-12489, Germany*

[6]*Potsdam Institute for Climate Impact Research, Telegraphenberg, Potsdam D-14415, Germany*

[7]*Institute for Complex Systems and Mathematical Biology, University of Aberdeen, Aberdeen AB24 3FX, United Kingdom*

(Received 31 January 2012; published 23 May 2012)

The influences of spatial frequency distributions on complete amplitude death are explored by studying an array of diffusively coupled oscillators. We found that with all possible sets of spatial frequency distributions, the two critical coupling strengths ϵ_{c1} (lower-bounded value) and ϵ_{c2} (upper-bounded value) needed to get complete amplitude death exhibit a universal power law and a log-normal distribution respectively, which has long tails in both cases. This is significant for dynamics control, since large variations of ϵ_{c1} and ϵ_{c2} are possible for some spatial arrangements. Moreover, we explore optimal spatial distributions with the smallest (largest) ϵ_{c1} or ϵ_{c2}.

DOI: 10.1103/PhysRevE.85.056211 PACS number(s): 05.45.Xt

I. INTRODUCTION

The collective behavior of a large number of coupled oscillators has been widely explored for better understanding the dynamics of many natural systems [1,2]. Many emergent phenomena such as synchronization [3–5], hysteresis, amplitude death [6–9], and oscillator death [10–13] have attracted the interest of scientists. Among them, synchronization dynamics has been most widely studied, and various types of synchronous dynamics, such as complete synchronization [3], phase synchronization [14], generalized synchronization [15], and antiphase synchronization [16] have been reported in many fields. Meanwhile, another emergent phenomenon of strong relevance is amplitude death (AD), which is realized by a suppression of the oscillating dynamics. AD plays a crucial role in many real systems, such as chemical reactions, synthetic genetic networks [17–19], and coupled laser systems [20]. Various mechanisms of AD have been so far reported as delay [21] in coupling due to a finite propagation of the signal, dynamic coupling [22], coupling through conjugate variables [23,24], nonlinear coupling [9], and parameter mismatches [25–27].

Since parameter mismatches are omnipresent in the real world, the occurrence of AD in coupled nonidentical oscillator systems has been analyzed in many cases. Effects of topological properties on partial AD dynamics (PAD) (defined as a situation where parts of oscillators in the coupled system become AD) were explored in small world networks [25], where randomly rewired links are found helpful to eliminate PAD existing in a ring of regularly coupled oscillators. Transition processes were also explored in a ring [26] (or in scale-free networks [27]) of coupled nonidentical oscillators. Rich dynamics have been observed when the coupled system transits from PAD to complete AD (CAD) (all coupled oscillators get to AD) owing to the competition between frequency mismatches and coupling-induced synchronization clusters. In [28], the authors considered a special case where the natural frequencies of the oscillators are distributed in a regular monotonic trend. PAD was found where AD occurs only in regions with a relatively large gradient of natural frequencies due to the competition between the synchronous clusters and the frequency mismatches. Moreover, the desynchronization-induced PAD can be weakened considerably by introducing random frequency deviations into a linear trend of frequency distribution.

However, the spatial frequency distributions of coupled oscillators are not generally limited to a linear trend distribution as in [28] or just adding small deviations; their spatial frequency distribution may have various sets of rearrangements. The purpose of this paper is to study the formation of CAD and the effects of general spatial frequency distributions on CAD. It is natural to raise then the following questions. How does the spatial frequency distribution influence CAD of an array of coupled oscillators? What kind of spatial frequency distribution is beneficial for CAD in an array of coupled nonidentical oscillators? To answer those questions, CAD dynamics of an array of coupled nonidentical Landau-Stuart oscillators with no-flux boundary conditions (NBCs) are explored. Here we study the effects of different spatial frequency rearrangements on the critical coupling constant ϵ_{c1} and ϵ_{c2} for CAD in Eq. (1). It is expected that each spatial arrangement of frequencies has different critical coupling constants ϵ_{c1} and ϵ_{c2} for CAD. Interestingly, all ϵ_{c1} and ϵ_{c2} for all sets of possible spatial frequencies distributions obey power-law and log-normal distribution, respectively, which both have long tails. Therefore, the rearrangement of the spatial frequency distribution has a strong influence on the critical value of the coupling constant needed for CAD. In particular, arrangements with the smallest (largest) ϵ_{c1} and ϵ_{c2} are found.

*wqliujx@gmail.com

The remainder of this paper is organized as follows. In Sec. II, we give our model for CAD. We will analyze the stabilities of CAD in our model with linear and random spatial frequency distributions in Sec. III. Finally, Sec. IV is devoted to some brief discussions and conclusions.

II. MODELS

The coupled system consisting of Landau-Stuart oscillators is presented as follows:

$$\dot{z_j}(t) = (1 + i\omega_j + |z_j(t)|^2)z_j(t) + \epsilon[z_{j+1}(t) + z_{j-1}(t) - 2z_j(t)], \quad j = 1,\ldots,N, \tag{1}$$

where i is the imaginary, and $z_j(t)$ is a complex variable. Here the boundary conditions are arbitrarily set as NBC with $z_{N+1}(t) = z_N(t), z_0(t) = z_1(t)$. For simplicity, we suppose that the coupled oscillators initially have a regular monotonic trend of the natural frequency distribution w_j. Without coupling ($\epsilon = 0$), each oscillator has an unstable focus at the origin $|z_j| = 0$ and an attracting limit cycle $z_j(t) = e^{i\omega_j t} = x(t) + iy(t)$ with a different oscillating frequency ω_j. Without disorder of the linear frequency distributions, the increment of the coupling constant drives the coupled system from PAD (happened in the middle part of arrays) to CAD (there is a critical coupling constant ϵ_{c1}, and CAD occurs when $\epsilon \geqslant \epsilon_{c1}$), which is similar to the results in [28]. When the coupling constant $\epsilon > \epsilon_{c2}$, the coupled system becomes oscillating again in a stable synchronous state (phase locking) [25,26], i.e., CAD is destroyed.

III. RESULTS

A. Linear frequency distributions

Let us first consider the coupled oscillators with linearly distributed natural frequencies ω:

$$w_j = \omega_0 + (j-1)\delta\omega, \quad j = 1,2,\ldots,N, \tag{2}$$

where ω_0 is arbitrarily set as 1 and $\delta\omega$ is the frequency mismatch of neighbored oscillators. The stability of CAD is analyzed by linearizing Eq. (1) at $|z_j| = 0, j = 1,2,\ldots,N$. If a perturbation $\eta_j(t)$ is introduced into the fixed point $|z_j| = 0, j = 1,2,\ldots,N$, then the evolution of the perturbations can be governed by the following equation:

$$\dot{\eta}_j(t) = (1 - m_j\epsilon + i\omega_j)\eta_j(t) + \epsilon\eta_{j+1}(t) + \epsilon\eta_{j-1}(t). \tag{3}$$

With the definition of the column vector $\eta(t) = [\eta_1(t), \eta_2(t),\ldots,\eta_n(t)]'$ (where $'$ is the transpose symbol), Eq. (3) can be rewritten as follows:

$$\dot{\eta}(t) = H\eta(t), \tag{4}$$

where H can be described as follows for a fixed boundary condition:

$$H = \begin{pmatrix} 1-m_1\epsilon+i\omega_1 & \epsilon & \cdots & \\ \epsilon & 1-m_2\epsilon+i\omega_2 & \epsilon & \\ & \epsilon & 1-m_3\epsilon+i\omega_3 & \epsilon \\ & \cdots & \cdots & \cdots \\ & \cdots & \epsilon & 1-m_N\epsilon+i\omega_N \end{pmatrix}$$

where the blank areas of the matrix H are all zero, $m_1 = m_N = 1$, $m_j = 2$, $(j = 2,3,\ldots,N-1)$. Assume that H can be diagonalized by a matrix P,

$$P^{-1}HP = \mathrm{diag}(\lambda_0,\lambda_1,\ldots,\lambda_{N-1}), \tag{5}$$

where $\lambda_k, k = 0,1,\ldots,N-1$ are the eigenvalues of H. A necessary condition for stable CAD of Eq. (2) is that all real parts of the eigenvalues $\mathrm{Re}(\lambda_k) < 0, k = 0,1,\ldots,N-1$. Therefore, the region of the AD state is completely determined by the critical lines of all $\mathrm{Re}(\lambda_k) \leqslant 0, k = 0,1,\ldots,N-1$. When $0 < N \leqslant 2$, the parameter region for CAD was presented theoretically as in [29]. When $N = 3$, the real parts of all eigenvalues can be presented analytically as in Eq. (6):

$$\mathrm{Re}(\lambda_1) = 1 - 4\epsilon/3 + \frac{1}{3}\sqrt[3]{A} - \frac{3\delta\omega^2 - 7\epsilon^2}{3\sqrt[3]{A}},$$
$$\mathrm{Re}(\lambda_2,3) = 1 - 4\epsilon/3 - \frac{1}{6}\sqrt[3]{A} + \frac{3\delta\omega^2 - 7\epsilon^2}{6\sqrt[3]{A}}, \tag{6}$$
$$A = 3\sqrt{3}\sqrt{\delta\omega^6 - 4\delta\omega^4\epsilon^2 + 23\delta\omega^2\epsilon^4 - 9\epsilon^6} - 9\delta\omega^2\epsilon - 10\epsilon^3.$$

Let $\mathrm{Re}(\lambda_i) = 0, (i = 1,2,3)$, we can get then the critical lines for CAD theoretically as presented in Eqs. (7) and (8), which are noted with $L1$ and $L2$, respectively, in Fig. 1(a). The CAD domains in the parameter space $\epsilon \sim \delta\omega$ are the areas enclosed by $L1$ and $L2$ [Eqs. (7) and (8), respectively], which coincide well with the numerical results as the dotted areas in Fig. 1(a):

$$\delta\omega = \sqrt{\frac{6\epsilon^3 - 19\epsilon^2 + 16\epsilon - 4}{1-\epsilon}}, \tag{7}$$

$$\delta\omega = \sqrt{\frac{\epsilon^2 - 4\epsilon + 1}{2\epsilon - 1}}. \tag{8}$$

However, it is difficult to diagonalize the matrix H analytically for large N. The CAD dynamics of the coupled oscillators should then be explored by numerical simulations. The CAD domains in the $\epsilon \sim \delta\omega$ parameter space are numerically presented in Fig. 1(b) for $N = 9$. The AD domain of coupled oscillators are the top part of the V-like lines. For a given coupling strength ϵ (or the frequency mismatch $\delta\omega$), CAD can be realized when the frequency mismatch $\delta\omega$ (or the coupling strength ϵ) is larger than a critical value. When $\delta\omega < \delta\omega_c$ ($\delta\omega_c = 1.2106$ for $N = 3$, the tip of the V-shaped lines, is related to the system size N), the coupled system transits from a noncoherent state to a synchronous state directly without a CAD state with the increment of the coupling strength.

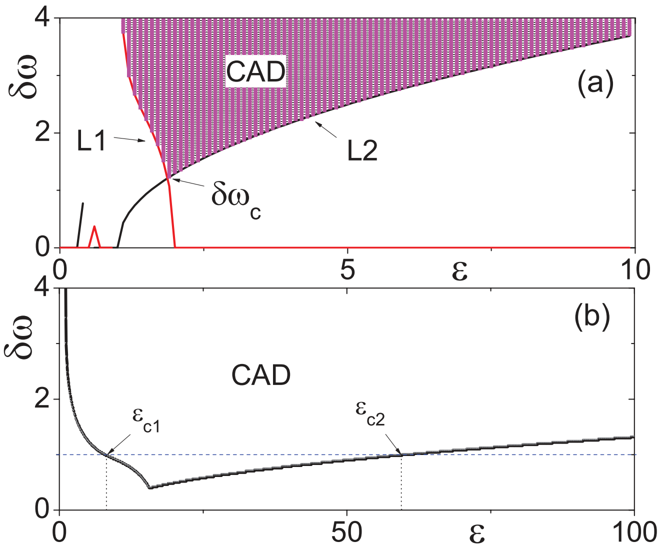

FIG. 1. (Color online) (a) The CAD domain of numerical results in the parameter space $(\epsilon,\delta\omega)$ and the theoretical critical lines of CAD for $N = 3$ coupled oscillators with linear trend of frequency distribution. The V-type areas enclosed by $L1$ [Eq. (7)] and $L2$ [Eq. (8)] are the CAD domains where the minimum frequency mismatch of the neighbored oscillator necessary for CAD is $\delta\omega_c = 1.2106$. (b) The CAD domain of numerical results for $N = 9$.

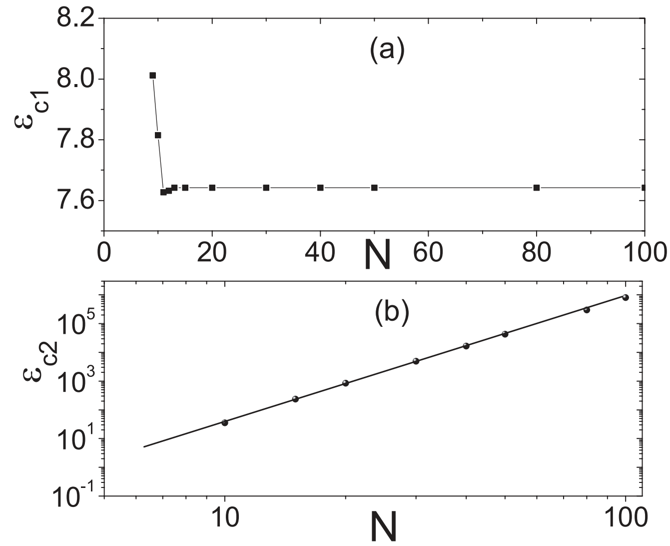

FIG. 2. (a) and (b) The system size effects on the critical values ϵ_{c1} and ϵ_{c2}, respectively, for coupled oscillators with linear frequency distributions.

When $\delta\omega > \delta\omega_c$, CAD is realized in the interval of $[\epsilon_{c1},\epsilon_{c2}]$. There are two critical values of ϵ_{c1} and ϵ_{c2} which can be calculated according to Eqs. (7) and (8), respectively, for given $\delta\omega$ for $N = 3$. These results coincide with the results in [29], where CAD is analytically found in the parameter region $\epsilon \in [1,(1 + \delta\omega^2/4)/2]$ when $\delta\omega_c \geqslant 2$ for $N = 2$. However, the coupled system is in a noncoherent state or in a partial synchronization (or coexisting with PAD) state for $\epsilon < \epsilon_{c1}$ and in a synchronous state for $\epsilon > \epsilon_{c2}$. We have to explain that ϵ_{c1} decreases to a constant value ϵ_0 ($\epsilon_0 \approx 1.0$, which coincides with the analytic results in [29]) when the value of $\delta\omega$ increases. Moreover, we find different scale effects of the critical values of ϵ_{c1} and ϵ_{c2} in dependence on the system size N for a given $\delta\omega$. ϵ_{c1} decreases linearly to a constant value 7.642, while ϵ_{c2} has a power law relation to the system size N. ϵ_{c1} and ϵ_{c2} versus the system size N for $\delta\omega = 1$ in Eq. (2) are presented in Figs. 2(a) and 2(b), respectively.

B. Random frequency distributions

To investigate effects of the spatial distribution of the natural frequencies on CAD, we rearrange the coupled oscillators which are originally in a linear frequency distribution by randomly exchanging their spatial sites. An arbitrary spatial site arrangement is denoted by a set $A = \{a(1),a(2), \ldots ,a(N)\}$ whose elements are permutations of $\{1,2, \ldots ,N\}$. Then the frequency distribution of an arbitrary spatial configuration of the frequency distribution can be described as $\hat{\omega}_{a(j)} = \omega_j,(j = 1,2, \ldots ,N)$. The total number of independent possible spatial arrangements for N coupled oscillators is $N!$. Since $N!$ increases so quickly with N, comprehensive computations of ϵ_c for all different configurations is impossible for large N. Fortunately, we find that the distributions are stable for randomly arranged large numbers of samples. The critical coupling constants ϵ_{c1} and ϵ_{c2} for CAD are expected to be varied for different sets of spatial arrangements. To better explore the critical coupling constants ϵ_{c1} and ϵ_{c2} for all possible sets of spatial frequency distributions, we have to select a proper value of $\delta\omega$ due to reasons listed below:

(1) If $\delta\omega$ is too large, the critical coupling strength ϵ_{c1} for CAD is almost constant for all possible spatial rearrangements.

(2) When the value of $\delta\omega$ is selected near the tip of the V-like critical line, most of the samples of the site rearrangements transit to a synchronous state directly from a non-CAD state.

For simplicity, we first consider coupled oscillators with a rather small size $N = 9$ and $\delta\omega = 2$ (not limited to those given values). The frequencies are first set according to Eq. (2). Intuitively, one may expect that the distribution of the critical values of ϵ_{c1} and ϵ_{c2} for all spatial arrangements would be a normal distribution, since the roughness R of the frequency distribution [defined as $R = \Sigma_{i=1}^{N-1} \frac{1}{N-1}(\omega_{i+1} - \omega_i)^2$] for all possible spatial arrangements is found to obey a normal distribution (results are not presented here). However, our research uncovers an opposite result: the distributions of all ϵ_{c1} and ϵ_{c2} for all sets of spatial frequency distributions are well fitted by a power law function and log-normal function, respectively, as plotted in Figs. 3(a) and 3(b). The power law function is described as

$$P(\epsilon_{c1}) \propto \epsilon_{c1}^{\gamma}, \tag{9}$$

where $\gamma = -3.1$. The log-normal function has the form

$$P(\epsilon_{c2}) = \frac{1}{\beta\epsilon_{c2}\sqrt{2\pi}} e^{-\frac{[\ln(\epsilon_{c2})-\lambda]^2}{2\beta^2}}, \tag{10}$$

which has the mean $\langle\epsilon_{c2}\rangle = e^{(\lambda+\beta/2)}$ with $\lambda = 3.441$ and $\beta = 0.162$. It is notable that both the power law distribution and the log-normal distribution have a long tail and are very common in many systems, e.g., scale-free networks, geology and mining, medicine, mining, medicine, climatology, and aerobiology, economics, etc. [30–34]. What should be mentioned is that there is a peak noted B in Fig. 3(b) which is located near the

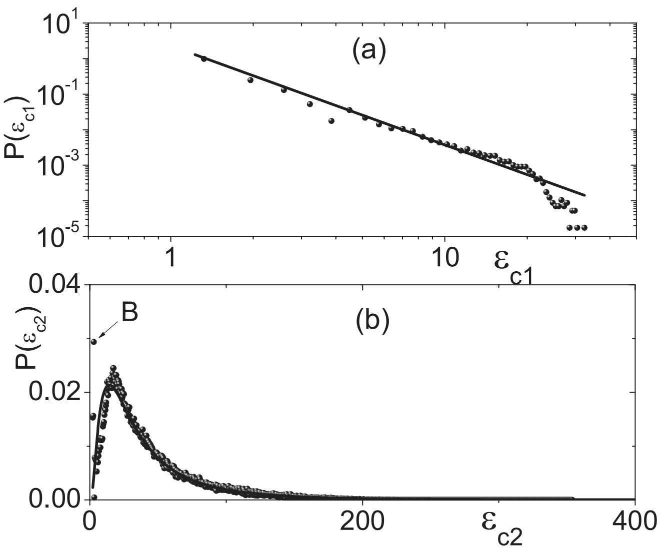

FIG. 3. (a) The possibility distribution of the critical value of ϵ_{c1} for all possible rearrangements of frequencies (dots). The black line is a fitted power law function with parameter $\gamma = -3.1$. (b) The possibility distribution of the critical value of ϵ_{c2} (dots). The black line is a fitted log-normal function with parameter $\lambda = 3.41$, $\beta = 0.85$. There are large numbers of spatial arrangements with the smallest ϵ_{c2} (noted with B).

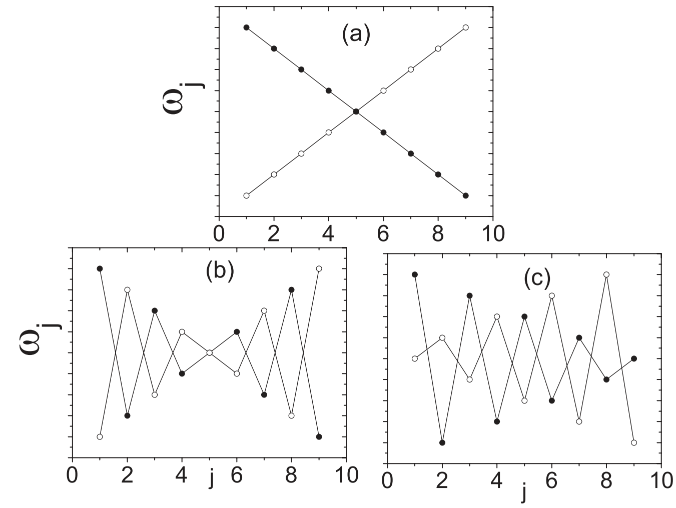

FIG. 4. Two sets of spatial frequency distributions (solid dots and circle dots) with which the coupled oscillators have stable CAD for the smallest (largest) ϵ_c. j's are the site numbers of oscillators. ω_j is the frequency of oscillator j. CAD can be realized (a) with the largest ϵ_{c2}; (b) with the smallest ϵ_{c1}; (c) with the smallest ϵ_{c2} and the largest ϵ_{c1}.

smallest $\epsilon_{c1} = 1.05$. The height of peak B is related to $\delta\omega$. If $\delta\omega$ increases, then the height of peak B increases. Actually, this is because some spatial arrangements have an effect of enlarging the average frequency mismatch $\delta\omega$. Therefore, if the average frequency mismatch of the arrangements is larger than $\delta\omega_c{}'$, then system (1) will get to CAD for the smallest $\epsilon_{c1} = 1.05$. Meanwhile, there are also some arrangements that have no CAD state but transit to a synchronous state if their equal effects of average frequency mismatch are below $\delta\omega_c$, as noted in Fig. 1(a).

It is curious to know what kinds of spatial distribution have the smallest or largest critical coupling constant for CAD. According to the results listed in Table I, we find that the spatial distributions with the smallest or largest critical coupling are quite different for ϵ_{c1} and ϵ_{c2}, respectively.

When the spatial arrangement of site indices are presented as $A = \{9,2,7,4,5,6,3,8,1\}$ or $A = \{1,8,3,6,5,4,7,2,9\}$, CAD can be realized with the smallest ϵ_{c1}. The frequency distributions are presented in Fig. 4(b) with the order of linearly increasing (decreasing) site indices $a(j)$.

When the spatial arrangement of site indices are presented as $A = \{9,7,5,3,1,2,4,6,8\}$ or $A = \{8,6,4,2,1,3,5,7,9\}$, CAD can be realized with the largest ϵ_{c1} and smallest ϵ_{c2}. The frequency distributions are presented in Fig. 4(c) with the order of linearly increasing (decreasing) site indices $a(j)$.

TABLE I. Spatial arrangements with the smallest and largest critical coupling constant.

	ϵ_{c1}	ϵ_{c2}
Spatial distribution with smallest ϵ_c.	Fig. 4(b)	Fig. 4(c)
Spatial distribution with largest ϵ_c.	Fig. 4(c)	Fig. 4(a)

For the largest ϵ_{c2}, the spatial arrangement of site indices are presented as $A = \{1,2,3,4,5,6,7,8,9\}$ or $A = \{9,8,7,6,5,4,3,2,1\}$. The frequency distributions are presented in Fig. 4(a) with the order of linearly increasing (decreasing) site indices $a(j)$.

It is well known that CAD and synchronization are both the results of competitions between spatial inhomogeneity and the coupling-caused order [26]. In the case of only two coupled nonidentical oscillators [29], the system transits from a phase-shifting state ($\epsilon < 1$) to a phase-locking state and finally reaches a CAD state (under the condition of $\delta\omega > 2$ and $1 < \epsilon < (1 + \delta\omega^2/4)/2$) with the increment of coupling constant. When the frequency mismatch is small $\delta\omega < 2$, the coupled system will transit to synchronization. However, the transition process may be more complex for an array ($N > 2$) of coupled nonidentical oscillators. With the competition of frequency mismatch of oscillators and spatial location, the formation of some synchronous clusters (oscillators in one cluster have the same frequencies) are expected. They combine with each other and become larger clusters. If the frequency arrangement is helpful to form one synchronous cluster, then a larger critical coupling constant ϵ_{c1} is needed to get CAD and a smaller critical coupling constant ϵ_{c2} is needed to leave CAD, since the synchronous clusters may delay or even prevent CAD. A detailed analysis on synchronization with the influences of the spatial frequency distributions is presented in [35]. If the frequency arrangement is beneficial to form two clusters with large average frequency mismatches and an equal number of oscillators, then a smaller ϵ_{c1} can realize CAD. In order to verify the above speculations, we take the spatial frequency arrangement as shown in Figs. 4(b) and 4(c) which has smallest and largest ϵ_{c1}, respectively. We carefully calculate the average frequency $\langle\omega_j\rangle$ [defined in Eq. (11)] of each oscillator versus ϵ as shown in Figs. 5(a) and 5(c),

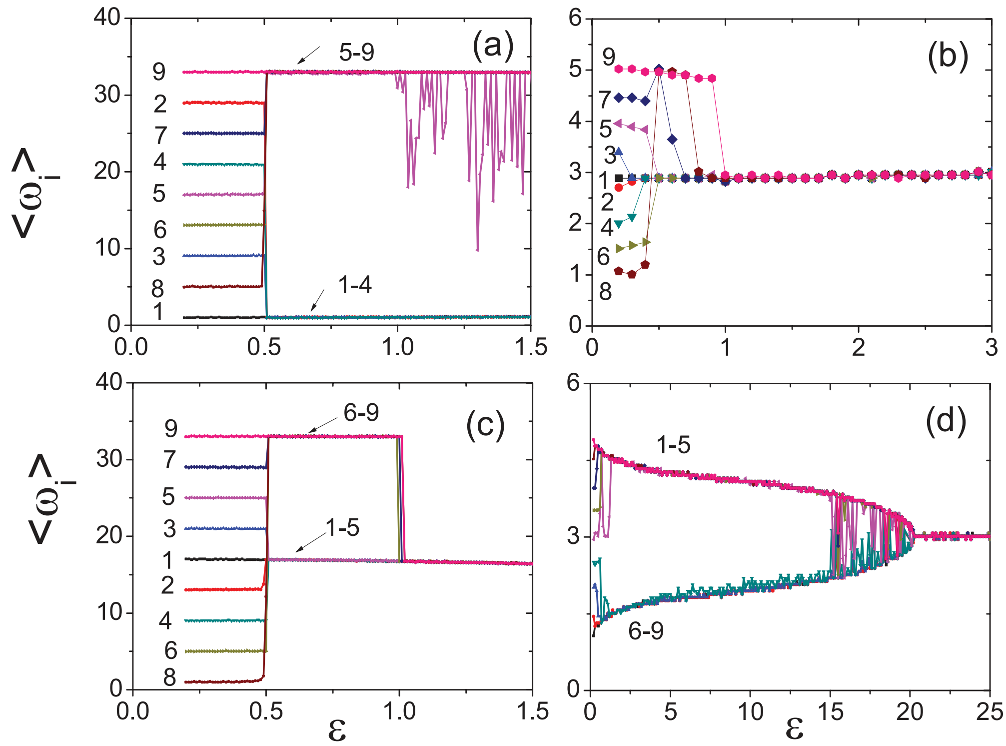

FIG. 5. (Color online) Average frequency of coupled nonidentical oscillators versus coupling constant. (a, c) With the spatial arrangement as in Figs. 4(b) and 4(c), respectively ($\delta\omega = 4$). (b, d) with the spatial arrangement as in Figs. 4(c) and 4(a), respectively ($\delta\omega = 0.5$).

respectively:

$$\langle\omega_j\rangle = \lim_{T\to\infty}\frac{1}{T}\int_0^T \dot{\theta}_j(t)dt. \tag{11}$$

This way we find the following:

(1) In Fig. 5(a), the oscillators $1-4$ are combined to a synchronous cluster with $\langle\omega_j\rangle = 1$, while the oscillators $5-9$ form another synchronous cluster with $\langle\omega_j\rangle = 33$. Obviously, the two synchronous clusters have the largest average frequency mismatches, which results in the smallest ϵ_{c1} for CAD.

(2) In Fig. 5(c), the oscillators $1-5$ are combined to a synchronous cluster with $\langle\omega_j\rangle = 16.5$ and the oscillators $6-9$ form another synchronous cluster with $\langle\omega_j\rangle = 33$. Finally, the two clusters are combined to one cluster with $\langle\omega_j\rangle = 16.5$ at $\epsilon = 1.02$. Both synchronous clusters with half of the maximum frequency mismatch and the combined cluster may delay or even prevent of CAD. Therefore, the largest ϵ_{c1} is necessary for CAD.

Similarly, according to the average frequency $\langle\omega_j\rangle$ of the coupled system with spatial frequency arrangement in Figs. 4(c) and 4(a) as shown in Figs. 5(b) and 5(d), respectively, we find that one synchronous cluster is formed at $\epsilon_c = 1.01$ for the spatial frequency arrangement in Fig. 4(c), while it is formed at $\epsilon_c = 20.6$ for the spatial frequency arrangement in Fig. 4(a).

IV. DISCUSSION AND CONCLUSION

In conclusion, we have comprehensively studied the influences of the spatial frequency distribution on CAD in an array of diffusively coupled nonidentical oscillators and uncover a regime of the spatial frequency distribution on CAD. Two different critical coupling constants ϵ_{c1} and ϵ_{c2} for getting CAD are theoretically found related to the frequency mismatches of neighbored oscillators in two coupled oscillators in [29]. In an array of coupled nonidentical oscillators, the rearrangement of the spatial frequency distribution can considerably diversify the values of ϵ_{c1} and ϵ_{c2}, since ϵ_{c1} obeys a power law distribution, while ϵ_{c2} obeys a log-normal one for all possible samples of spatial configurations. Compared to the normal distribution, the long tail characteristics of the power law distribution and the log-normal distribution are more significant from the viewpoint of control, since there exist some values which are far away from the mean of the critical values. Therefore, some arrangements of spatial frequency are possible far away from the CAD state for a given coupling constant. The results would be valuable from a practical standpoint with regard to controlling the dynamics. Moreover, the optimal spatial distributions are found for the smallest (largest) ϵ_c which are found to be related to the competition of synchronous dynamics and spatial mismatches. This may be helpful for understanding desynchronization patterns in coupled systems.

What should be mentioned is that the results are not inclusive in NBC but also in periodical boundary conditions. Meanwhile, the original distribution is not limited to a linear trend of the frequency distribution ($\delta\omega_j$ is constant), and the distributions of ϵ_{c1} and ϵ_{c2} are stable kept when $\delta\omega_j$ are presented in a random distribution. Research on the effects of spatial frequencies may be promising in exploring pattern formation in two-dimensional coupled oscillators, or even in complex networks where rich dynamics are expected under the competition between the spatial frequency distributions and the topological structures.

ACKNOWLEDGMENTS

This paper was supported by the National Natural Science Foundation of China (Grants No. 61104152, No. 10947117, No. 11062002, No. 11147179 and No. 11171125), Fundamental Research Funds for the Central Universities (Grants No. 2010RC01 and No. 2011QN161), the Science and Technology Project of Jiangxi Province (Grants No. GJJ12330 and No. 2010GQW0021), the Alexander von Humboldt Foundation of Germany, and IRTG 1740 (DFG and FAPESP).

[1] A. T. Winfree, *The Geometry of Biological Time* (Springer-Verlag, New York, 1980).
[2] A. Pikovsky, M. Rosenblum, and J. Kurths, *Synchronization: A Universal Concept in Nonlinear Dynamics* (Cambridge University Press, Cambridge, England, 2001).
[3] L. M. Pecora and T. L. Carroll, Phys. Rev. Lett. **64**, 821 (1990).
[4] A. Arenas, A. Díaz-Guilera, J. Kurths, Y. Moreno, and C. Zhou, Phys. Rep. **469**, 93 (2008).
[5] S. Boccaletti, J. Kurths, G. Osipov, D. L. Valladares, and C. S. Zhou, Phys. Rep. **366**, 1 (2002).
[6] G. B. Ermentrout, Physica D **41**, 219 (1990).
[7] R. E. Mirollo and S. H. Strogatz, J. Stat. Phys. **60**, 245 (1990).
[8] V. Resmi, G. Ambika, and R. E. Amritkar, Phys. Rev. E **84**, 046212 (2011).
[9] A. Prasad, M. Dhamala, B. M. Adhikari, and R. Ramaswamy, Phys. Rev. E **81**, 027201 (2010).
[10] W. Zou, C. Yao, and M. Zhan, Phys. Rev. E **82**, 056203 (2010).
[11] W. Zou, J. Lu, Y. Tang, C. Zhang, and J. Kurths, Phys. Rev. E **84**, 066208 (2011).
[12] J. J. Surez-Vargas, J. A. Gonzlez, A. Stefanovska, and P. V. E. Mcclintock, Europhys. Lett. **85**(3), 38008 (2009).
[13] M. Dolnik and I. R. Epstein, Phys. Rev. E **54**, 3361 (1996).
[14] M. G. Rosenblum, A. S. Pikovsky, and J. Kurths, Phys. Rev. Lett. **76**, 1804 (1996).
[15] N. F. Rulkov, M. M. Sushchik, L. S. Tsimring, and H. D. I. Abarbanel, Phys. Rev. E **51**, 980 (1995).
[16] W. Q. Liu, J. H. Xiao, X. L. Qian, and J. Z. Yang, Phys. Rev. E **73**, 057203 (2006).
[17] E. Ullner, A. Zaikin, E. I. Volkov, and J. Garcia-Ojalvo, Phys. Rev. Lett. **99**, 148103 (2007).
[18] A. Koseska, E. Volkov, and J. Kurths, Europhys. Lett. **85**, 28002 (2009).
[19] A. Koseska, E. Volkov, and J. Kurths, Chaos **20**, 023132 (2010).
[20] M. D. Wei and J. C. Lun, Appl. Phys. Lett. **91**, 061121 (2007).
[21] D. V. Ramana Reddy, A. Sen, and G. L. Johnston, Phys. Rev. Lett. **80**, 5109 (1998).
[22] K. Konishi, Phys. Rev. E **68**, 067202 (2003).
[23] R. Karnatak, R. Ramaswamy, and A. Prasad, Phys. Rev. E **76**, 035201(R) (2007).
[24] W. Zou, X. G. Wang, Q. Zhao, and M. Zhan, Fron. Phys. China **4**, 97 (2009).
[25] Z. Hou and H. Xin, Phys. Rev. E **68**, 055103(R) (2003).
[26] J. Yang, Phys. Rev. E **76**, 016204 (2007).
[27] W. Liu, X. Wang, S. Guan, and C.-H. Lai, New J. Phys. **11**, 093016 (2009).
[28] L. Rubchinsky and M. Sushchik, Phys. Rev. E **62**, 6440 (2000).
[29] D. G. Aronson, G. B. Ermentrout, and N. Kopell, Physica D **41**, 403 (1990).
[30] A.-L. Barabsi and R. Albert, Science **286**, 509 (1999).
[31] E. Limpert, W. A. Stahel, and M. Abbt, BioScience **51**, 341 (2001).
[32] C. Castellano, S. Fortunato, and V. Loreto, Rev. Mod. Phys. **81**, 591 (2009).
[33] M. Medo, G. Cimini, and S. Gualdi, Phys. Rev. Lett. **107**, 238701 (2011).
[34] K. Tokita, Phys. Rev. Lett. **93**, 178102 (2004).
[35] Y. Wu, J. H. Xiao, G. Hu, and M. Zhan, Europhys. Lett. **97**, 40005 (2012).